

Global gridded dataset of Heating and Cooling Degree Days under climate change scenarios

Jesus Lizana^{a,b,c,*}, Nicole D. Miranda^{b,c}, Sarah N. Sparrow^d,
David C.H. Wallom^{a,d}, Radhika Khosla^{a,b,e}, Malcolm McCulloch^{a,b,c}

^aZERO Institute, University of Oxford, Oxford OX2 0ES, United Kingdom.

^bFuture of Cooling Programme, Oxford Martin School, University of Oxford, Oxford OX1 3BD, United Kingdom.

^cEnergy and Power Group, Department of Engineering Science, University of Oxford, Oxford OX1 3PJ, United Kingdom.

^dOxford e-Research Centre, University of Oxford, Oxford OX13QG, United Kingdom.

^eSmith School of Enterprise and the Environment, School of Geography and the Environment, University of Oxford, Oxford OX1 3QY, United Kingdom.

*Corresponding author: jesus.lizana@eng.ox.ac.uk

Abstract

Accurate projections of heating and cooling demands are crucial for advancing towards the Sustainable Development Goals. Here, we present a global dataset of heating degree days (HDD) and cooling degree days (CDD) for three levels of global mean temperature rise above pre-industrial conditions—1.0°C (2006–2016), 1.5°C, and 2.0°C—regardless of the pathways leading to these warming scenarios. The dataset comprises 30 gridded maps (0.883° × 0.556° resolution) characterising climate variability through five statistical metrics per variable and scenario over a representative 10-year period. The dataset reveals a widespread decline in HDD and a pronounced, nonlinear increase in CDD, with the most significant shifts in climate intensity and adaptation needs emerging early in the warming trajectory. Furthermore, using the “middle-of-the-road” pathway SSP2-4.5 as a reference, the dataset indicates that the population experiencing extreme heat conditions (exceeding 3,000 CDD) is projected to nearly double if the 2.0°C threshold is reached, increasing from 23% (1.54 billion people) in 2010 to 41% (3.79 billion) by 2050, with the largest projected populations affected in India, Nigeria, Indonesia, Bangladesh, Pakistan, and the Philippines. This HDD–CDD dataset provides a robust foundation for integrating climate information into sustainability planning and development policy.

Introduction

Decarbonising heating and cooling energy systems is critical as these two end-uses dominate energy demand, are important sources of emissions, and are key to a range of sustainability goals^{1,2}. Heating currently accounts for approximately 45% of building emissions³, while space cooling is projected to expand more rapidly than any other building end-use, expected to be more than triple by 2050⁴. To inform sustainability and energy policy decisions, it is crucial to understand how climate change may affect building energy use and associated greenhouse gas emissions across temporal and spatial scales⁵. Developing more effective and resilient community mitigation and adaptation strategies for the built environment is imperative to achieving the global goal of net-zero carbon emissions by 2050⁶.

Heating Degree Days (HDD) and Cooling Degree Days (CDD) are widely used indicators to estimate heating and cooling demands globally, serving as key metrics for understanding energy needs across diverse climates and socio-economic contexts^{5,7}. They quantify the extent to which the daily mean temperatures deviate from a reference temperature threshold over a given period⁸. HDD are particularly relevant for assessing the implications of cold conditions in high-latitude and economically vulnerable regions, where energy poverty poses significant challenges. Likewise, CDD are instrumental in evaluating the impacts of extreme heat, especially in low-income areas where cooling access is limited, and vulnerability to heat stress is pronounced. Emerging research seeks to enhance these metrics by incorporating additional variables such as humidity, adaptive comfort thresholds, and behavioural factors to improve local relevance⁴. Despite these advancements, HDD and CDD remain indispensable, consistent, and scalable indicators for evaluating heating and cooling demands. Moreover, they enable comparability across existing studies, enhancing the usefulness of data for adaptation planning by providing more relevant and actionable insights.

Previous research on HDD and CDD has predominantly focused on global mapping using historical data^{9,10}, with some employing model-based climate projections to assess the climate change impacts in specific regions^{11–14} or globally under specific timeframes and emission pathways^{15,16}. The most recent global mapping of HDD and CDD under different climate change scenarios was produced by Spinoni et al. (2021)¹⁶. They generated global maps at a 0.44° × 0.44° resolution using outputs from 34 Coordinated Regional Climate Downscaling Experiment (CORDEX) simulations based on regional climate models (RCMs) driven by 20 global climate models (GCMs) from the Coupled Model Intercomparison Project Phase 5 (CMIP5). However, this dataset was not bias-corrected, lacked a historical baseline scenario (covering only 1.5 °C, 2 °C, 3 °C, and 4 °C above pre-industrial levels), and reported only ensemble medians and spreads—without capturing climate variability (e.g., P10, P90, or standard deviation). Moreover, the remaining previous studies have been mainly constrained to

specific temporal contexts and emissions pathways, making it challenging to compare datasets and scenarios due to the diverse range of methodologies and assumptions. This variability has created a substantial gap in forecasting and comparing current and future heating and cooling demands across global warming levels—from 1 °C (2006–2016) to 1.5 °C and 2.0 °C—independently of the timing of these changes. Key questions remain for adaptation planning, such as whether trends in HDD and CDD progress linearly or non-linearly, and whether these trends follow consistent patterns across countries or exhibit significant regional variations.

This study generates a global dataset of HDD and CDD for three global warming levels above pre-industrial conditions - 1.0°C (based on 2006-2016 observations), 1.5°C, and 2.0°C - regardless of when these occur, to evaluate the climate change implications for the heating and cooling sector globally. The temperature ensemble used to generate this dataset is characterised by (1) a high temporal resolution (6-hourly mean temperatures simulated with the HadAM4 climate model^{17,18}), (2) a large ensemble size (70 members over ten years), (3) bias-corrected outputs, (4) multiple statistical descriptors per grid cell to illustrate climate variability with 30 gridded maps, and (5) the representation of global mean temperature rise levels of 1.5°C and 2.0°C independently of the specific time at which these thresholds are reached. The HadAM4 climate model¹⁹ is particularly well-suited to the goals of this study, offering specific advantages over CMIP5 or CMIP6 models. While HadAM4 lacks interactive coupling to ocean and aerosol components, it is sufficiently memory-efficient to run on personal computers of volunteers using the climateprediction.net distributed computing platform²⁰. This computational efficiency enables the generation of very large, high-resolution ensembles using prescribed sea surface temperatures and greenhouse gas concentrations, an approach that would be prohibitively expensive to run on a standard supercomputer with most fully coupled Earth system models²¹. Its configuration is comparable to that of many CMIP6 and CMIP5 models, and its warming patterns are similar to the CMIP6 multi-model mean as reported by Lizana et al. (2024)¹⁷, ensuring a credible representation of climate dynamics. The HadAM4 configuration was selected for its efficiency in simulating stable global-mean temperature states¹⁷, or its demonstrated ability to represent extreme-season variability²¹. Moreover, the bias correction is also necessary because, unlike other studies such as Spinoni et al. (2021)¹⁶, it ensures that the results are not systematically skewed by model-specific errors, thereby improving the reliability and comparability of the findings. As a result, the bias-corrected HadAM4-based temperature ensemble used in this study features a large ensemble size (more than double those typically available in CMIP5 or CMIP6), high spatiotemporal resolution (6-hourly mean temperatures rather than daily variables), and the ability to represent global mean temperature rise levels of 1.5°C and 2.0°C above pre-industrial conditions independently of the specific timing at which these thresholds are reached. By decoupling the analysis from specific time horizons and focusing on global mean temperature rise thresholds, the dataset offers a unique, policy-relevant perspective on

climate impacts. This approach allows decision-makers and researchers to assess adaptation needs and infrastructure resilience irrespective of when these warming levels are reached, making it particularly valuable for long-term planning under uncertainty.

The three global warming levels adhere to the half a degree additional warming, prognosis and projected impacts (HAPPI) experimental design protocol²², with the historical scenario between 2006 and 2016 representing a global mean temperature rise of 1.0°C. The general dataset builds upon recent contributions^{4,9,15,16,23}, generating here an enhanced, comprehensive statistical gridded dataset of 30 maps that capture climate variability through five statistical descriptors for each variable and scenario over a 10-year representative period: mean, median, 10th percentile, 90th percentile, and standard deviation. The resulting global maps of HDD and CDD were calculated using the dry bulb temperature, following the standard approach⁸. The final global gridded maps have a spatial resolution of 0.833° × 0.556° (longitude × latitude), covering the land surface area. They are available in NetCDF-4 file format (*.nc) at the Oxford University Research Archive (ORA) repository²⁴.

These maps serve as a key resource for estimating evolving thermal demands under various global warming levels and assessing adaptation priorities, including energy infrastructure and policy needs. The dataset also facilitates the evaluation of energy equity, understanding of socio-economic impacts, and informed guidance on investments in renewable energy systems and climate-resilient designs. By integrating this data with variables such as population growth, urbanisation, and technological advancements, it supports the development of targeted and sustainable solutions for a warming world.

The following sections detail the generated dataset and examine its immediate implications. Firstly, the 30 global maps are described, and subregional changes in mean HDD and CDD are statistically demonstrated. Secondly, the countries anticipated to witness the most significant variations in HDD and CDD are identified. Thirdly, the rate of change in CDD and HDD across all countries is normalised and compared. Finally, the implications of these findings for the population are explored using the 'middle of the road' projection scenario (SSP2-4.5) as an example.

Global gridded maps of HDD and CDD under three global warming levels.

Understanding changes in future heating and cooling needs is crucial for forecasting energy demand, optimising energy systems, and supporting climate adaptation efforts. Reliable data is essential for effective resource allocation and advancing sustainability initiatives.

The complete dataset produced in this study is summarised in the Extended Data Table 1. It comprises 30 global gridded maps, covering two variables— HDD and CDD —across three global mean temperature rise scenarios: 1.0°C (based on 2006-2016 observations), 1.5°C, and 2.0°C. For each variable and scenario, five statistical descriptors of the model ensemble are provided: mean, median, 10th percentile, 90th percentile, and standard deviation. This dataset represents the most comprehensive global mapping to date of heating and cooling needs, capturing the ensemble-based climate variability across global warming levels. All maps are provided at a spatial resolution of $0.833^\circ \times 0.556^\circ$ (longitude \times latitude) over the land surface, approximately 60 km at mid-latitudes.

Fig. 1 illustrates and statistically analyses the spatial distribution of mean HDD. Left figures a1-c1 show global maps of mean HDD for each climate scenario, calculated as the annual mean per grid cell using a 70-member ensemble over a 10-year period (700 annual simulations per scenario). Right panels a2–c2 display boxplots of HDD distributions across world regions, enabling a comparative assessment of regional heating demand under progressive global warming.

While the spatial maps provide a global overview of HDD patterns, differences between scenarios may appear subtle given the scale of global change. However, the boxplots clearly demonstrate a consistent decline in HDD across all regions as global mean temperature rises. This downward trend indicates a widespread reduction in heating demand, with the most pronounced decreases occurring in higher-latitude regions that have historically exhibited the highest HDD values. The ensemble-based approach enhances the robustness of these findings, underscoring the significant impact that even modest global warming can have on regional energy impact for heating.

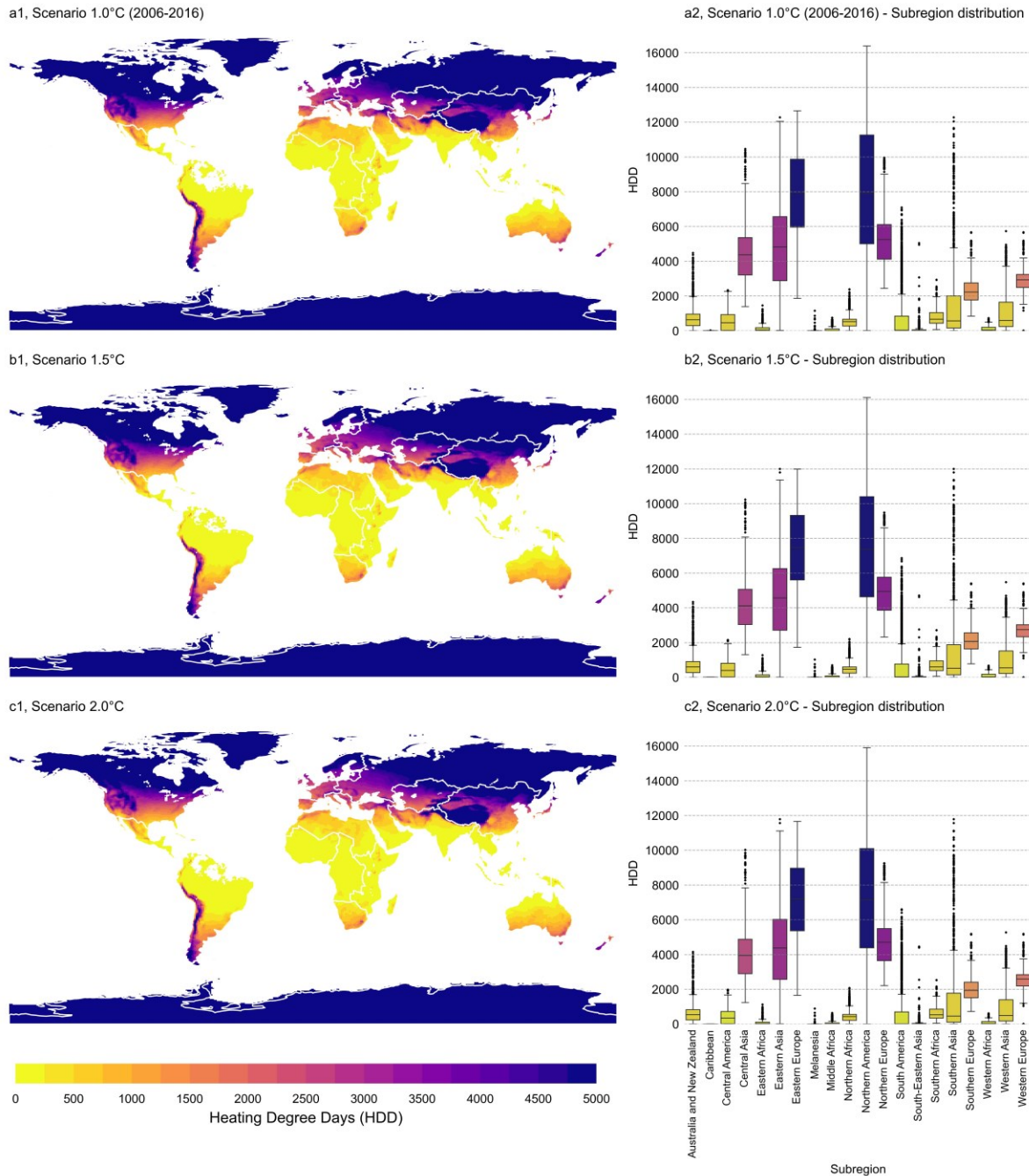


Figure 1 | Global mean HDD for three global warming scenarios: 1.0°C (2006-2016), 1.5°C and 2.0°C. a1, Global mean HDD for 1.0°C (historical scenario). **b1,** Global mean HDD for 1.5°C. **c1,** Global mean HDD for 2.0°C. Values are calculated as the annual mean HDD per grid across the ensemble of 70 members for 10 years per scenario, resulting in a total of 700 annual runs. Spatial resolution: 0.833 longitude and 0.556 latitude. The maps use subregion boundaries from Natural Earth. The boxplot shows the distribution of data by region, indicating the median (centre line), the interquartile range (IQR) (box, 25th–75th percentiles), whiskers extending to 1.5×IQR, and points beyond are plotted as outliers: **a2,** Boxplot of HDD distribution under the 1.0°C scenario (2006-2016). **b2,** Boxplot of HDD distribution under the 1.5°C scenario. **c2,** Boxplot of HDD distribution under the 2.0°C scenario.

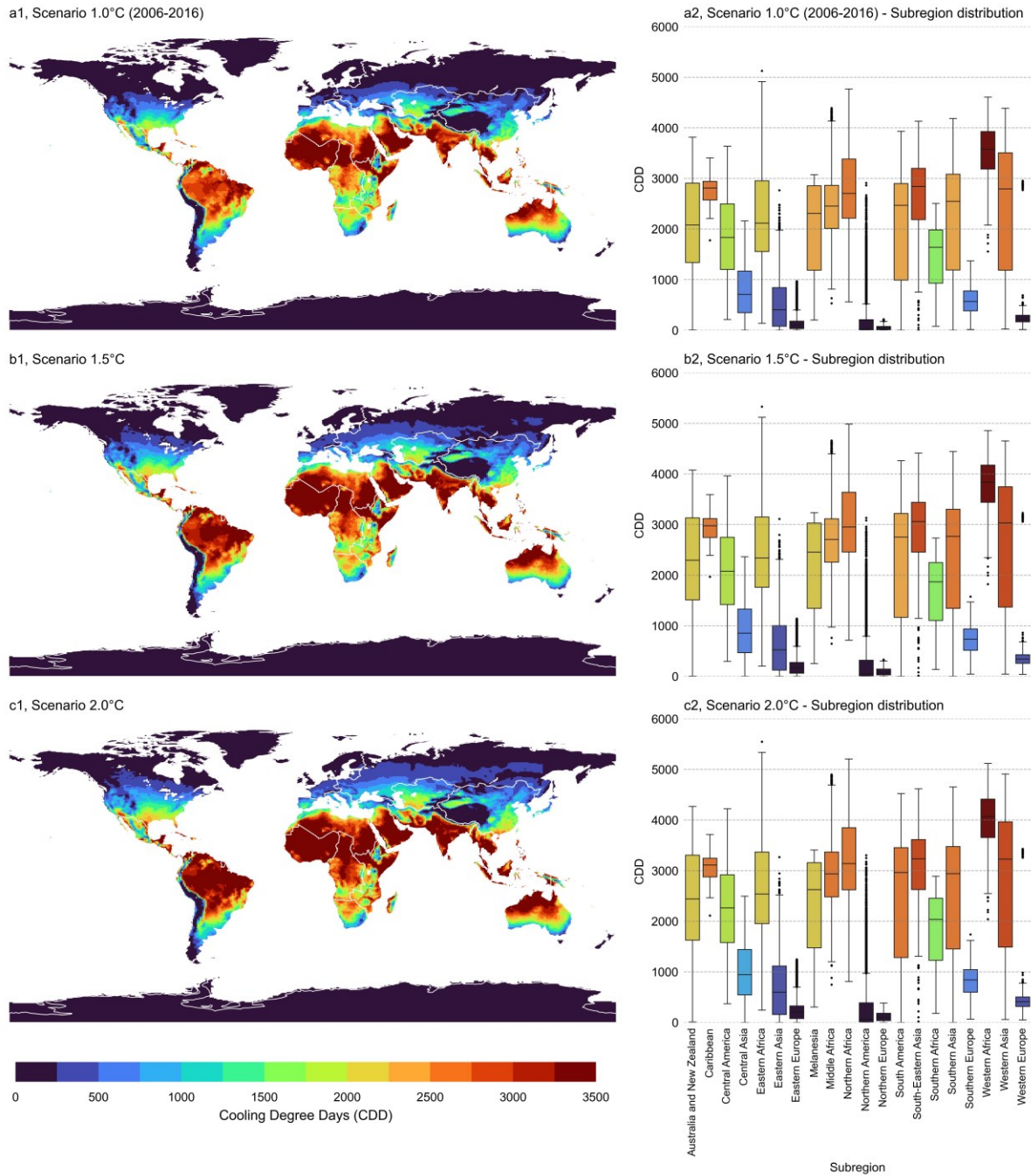


Figure 2 | Global mean CDD for three global warming scenarios: 1.0°C (2006-2016), 1.5°C and 2.0°C. **a1**, Global mean CDD for 1.0°C (historical scenario). **b1**, Global mean CDD for 1.5°C. **c1**, Global mean CDD for 2.0°C. Values are calculated as the annual mean CDD per grid across the ensemble of 70 members for 10 years per scenario, resulting in a total of 700 annual runs. Spatial resolution: 0.833 longitude and 0.556 latitude. The maps use subregion boundaries from Natural Earth. The boxplot shows the distribution of data by region, indicating the median (centre line), the interquartile range (IQR) (box, 25th–75th percentiles), whiskers extending to 1.5×IQR, and points beyond are plotted as outliers: **a2**, Boxplot of CDD distribution under the 1.0°C scenario (2006-2016). **b2**, Boxplot of CDD distribution under the 1.5°C scenario. **c2**, Boxplot of CDD distribution under the 2.0°C scenario.

In a similar approach, Fig. 2 shows and statistically analyses the spatial distribution of mean CDD, with left maps a1-c1 showing global mean CDD maps while right plots a2-c2 presenting regional boxplots for each warming scenario.

Again, while the spatial maps provide a broad overview of CDD patterns, the boxplots clearly reveal a consistent rise in CDD values across all regions as global temperatures increase. This upward trend signals a growing demand for cooling, particularly in lower-latitude regions already subject to high ambient temperatures. The results also indicate increasing disparities in cooling needs between regions. As with HDD, the ensemble-based methodology enhances the robustness of these findings, demonstrating that even modest warming can lead to significant changes in regional cooling requirements.

Additional descriptive statistics for the complete dataset are provided in Extended Data Table 1.

Global changes in Heating Degree Days

To gain an initial understanding of the dataset's implications, it is essential to identify the countries most likely to experience the most significant shifts in heating and cooling requirements. Table 1 lists the top twenty countries with populations exceeding 2 million that are projected to experience the most substantial changes in HDD from 1.0 to 2.0°C. Extended Data Fig. 1 illustrates the difference between historical mean HDD at 1.0°C and 1.5°C (Extended Data Fig. 1a), between 1.5°C and 2.0°C (Extended Data Fig. 1b), and between 1.0°C and 2.0°C (Extended Data Fig. 1c) global warming levels.

Table 1 | Countries with the highest absolute change in area-weighted mean HDD from 1.0°C (historical, 2006-2016) to 2.0°C scenario. The countries are ranked by the absolute change in their heating needs between the 1.0°C and 2.0°C scenarios. Delta HDD (Δ HDD) refers to the incremental/decremental change in area-weighted mean HDD per country.

	Top countries by ΔHDD₁₈	<i>ΔHDD₁₈ from 1.0 to 1.5°C</i>	<i>ΔHDD₁₈ from 1.5 to 2.0°C</i>	ΔHDD₁₈ from 1.0 to 2.0°C	<i>Relative Change (%) from 1.0 to 1.5°C</i>	<i>Relative Change (%) from 1.5 to 2.0°C</i>	<i>Relative Change (%) from 1.0 to 2.0°C</i>
1	Canada	-594	-256	-850	-7.0%	-3.3%	-10.0%
2	Russian Federation	-456	-296	-752	-5.6%	-3.9%	-9.3%
3	Finland	-337	-278	-614	-6.2%	-5.5%	-11.3%
4	Sweden	-312	-254	-566	-5.9%	-5.1%	-10.7%
5	Norway	-311	-242	-554	-5.5%	-4.6%	-9.9%
6	Mongolia	-263	-223	-486	-4.2%	-3.7%	-7.8%
7	United States	-278	-206	-484	-6.6%	-5.2%	-11.4%
8	Kyrgyzstan	-258	-195	-453	-4.2%	-3.3%	-7.4%
9	Austria	-249	-202	-451	-6.3%	-5.4%	-11.3%
10	Belarus	-242	-207	-449	-6.1%	-5.5%	-11.3%
11	Switzerland	-247	-201	-448	-5.7%	-4.9%	-10.3%
12	Armenia	-252	-184	-436	-6.3%	-4.9%	-10.9%
13	Lithuania	-231	-204	-436	-5.9%	-5.5%	-11.0%
14	North Korea	-246	-177	-423	-5.8%	-4.4%	-9.9%
15	China	-241	-181	-422	-5.3%	-4.2%	-9.3%
16	Kazakhstan	-250	-172	-421	-5.5%	-4.0%	-9.2%
17	Georgia	-244	-171	-415	-6.6%	-4.9%	-11.2%
18	Slovakia	-226	-183	-409	-6.7%	-5.9%	-12.2%
19	Czechia	-219	-187	-406	-6.4%	-5.8%	-11.8%
20	Tajikistan	-226	-179	-405	-3.5%	-2.9%	-6.3%

Countries with more than 2 million inhabitants in 2020 are listed. Annual HDD were calculated using a temperature baseline of 18°C. Delta (Δ) refers to the incremental (+) or decremental (-) change in the variable. The relative change (%) per country was calculated using area-weighted mean values rather than grid-based values. The bold column denotes the metric used for country ranking.

When analysing the top 20 countries with the largest change in heating needs as the world warms to 2.0°C, several key points are worth noting. Most of these twenty countries (18 out of 20) are among

the coolest regions in the world, as listed in SN3. In this context, Slovakia and Czechia take the place of Chile and Ukraine.

They are all regions from three main continents: North America, Europe, and Asia. The most considerable changes in area-weighted mean HDD are found in Canada, the Russian Federation, Finland, Sweden, and Norway, with reductions ranging from 554 to 850 HDD.

The decrease in heating needs is not linear in these regions. Most of the decrease in heating demand occurs before reaching the 1.5°C threshold, indicating that the most significant shifts in energy requirements happen in the early stages of warming rather than in a steady progression. This is evident in the comparison of Extended Data Fig. 1a and Fig. 1b, where the yellow areas are more widespread at the first warming threshold.

Changes in Cooling Degree Days

Table 2 ranks the top 20 countries with more than 2 million inhabitants that will experience the most significant absolute increase in area-weighted mean CDD from 1.0 to 2.0°C. Extended Data Fig. 2 illustrates the differences between historical mean CDD at 1.0°C and 1.5°C (Extended Data Fig. 2a), between 1.5°C and 2.0°C (Extended Data Fig. 2b), and between 1.0°C and 2.0°C (Extended Data Fig. 2c).

Table 2 | Countries with the highest absolute change in area-weighted mean CDD from 1.0°C (historical, 2006-2016) to 2.0°C scenario. The countries are ranked by the absolute change in their cooling needs between the 1.0°C and 2.0°C scenarios. Delta CDD (Δ CDD) refers to the incremental/decremental change in area-weighted mean CDD per country.

	Top countries by ΔCDD₁₈	<i>ΔCDD₁₈ from 1.0 to 1.5°C</i>	<i>ΔCDD₁₈ from 1.5 to 2.0°C</i>	<i>ΔCDD₁₈ from 1.0 to 2.0°C</i>	<i>Relative Change (%) from 1.0 to 1.5°C</i>	<i>Relative Change (%) from 1.5 to 2.0°C</i>	<i>Relative Change (%) from 1.0 to 2.0°C</i>
1	Central African Republic	293	266	560	+10.3%	8.5%	+19.6%
2	Nigeria	295	245	540	+8.9%	6.8%	+16.3%
3	South Sudan	285	251	536	+8.2%	6.7%	+15.4%
4	Laos	334	196	530	+15.6%	7.9%	+24.7%
5	Brazil	297	227	524	+11.4%	7.8%	+20.0%
6	Honduras	303	216	519	+14.4%	9.0%	+24.6%
7	Guatemala	292	225	516	+13.0%	8.9%	+23.0%
8	Burkina Faso	262	254	516	+6.8%	6.2%	+13.5%
9	Venezuela	294	214	508	+10.6%	6.9%	+18.3%
10	Paraguay	294	210	503	+11.9%	7.6%	+20.3%
11	Mali	250	253	503	+6.4%	6.0%	+12.8%
12	Thailand	303	197	499	+9.5%	5.6%	+15.7%
13	Chad	263	236	498	+7.3%	6.1%	+13.8%
14	Democratic Republic of The Congo	253	240	493	+11.1%	9.5%	+21.7%
15	Cameroon	264	228	491	+10.8%	8.4%	+20.0%
16	Benin	266	220	486	+7.8%	6.0%	+14.2%
17	Nicaragua	284	200	484	+10.5%	6.7%	+17.9%
18	Cambodia	294	189	482	+8.4%	5.0%	+13.8%
19	Congo	240	241	481	+9.5%	8.7%	+19.1%
20	Uganda	249	232	480	+12.8%	10.6%	+24.7%

Countries with more than 2 million inhabitants in 2020 are listed. Annual CDD were calculated using a temperature baseline of 18°C. Delta (Δ) refers to the incremental (+) or decremental (-) change in the variable. The relative value per country was calculated using area-weighted mean values rather than grid-based values. The bold column denotes the metric used for country ranking.

When analysing the top 20 countries with the largest increase in cooling needs under a 2.0°C rise in global mean temperature, several key points should be noted. In contrast to the changes in HDD, here, only 7 out of 20 countries are located in some of the hottest regions in the world (see all countries in

SN4). These regions are in Africa (Mali, Burkina Faso, Chad, South Sudan, Benin, Nigeria) and Asia (Cambodia).

The 20 countries with the most significant changes in CDD are also developing nations. They are all located near the equator or within tropical and subtropical latitudes, resulting in warm climates with high temperatures throughout the year. These shifts are expected to further strain the socio-economic development of these regions. Most of these countries are in Africa (Central African Republic, Nigeria, South Sudan, Burkina Faso, Mali, Chad, the Democratic Republic of the Congo, Cameroon, Uganda, Benin, Congo), whereas others are in South America (Brazil, Venezuela, Paraguay), Central America (Honduras, Guatemala, Nicaragua) and Southeast Asia (Laos, Thailand, Cambodia).

The largest increases in area-weighted mean CDD are observed in the Central African Republic, Nigeria, South Sudan, Laos, and Brazil, with increases of 524-560 CDD. These regions are projected to experience the most dramatic increase in cooling needs from 1.0°C to 2.0°C, as shown in Extended Data Fig. 2, necessitating substantial adaptation efforts.

Like HDD, most CDD changes occur before reaching the 1.5°C threshold across the top 20 countries, indicating that the most significant shifts in adaptation requirements to higher temperatures occur in the early stages of warming rather than in a steady progression. This is evident in the comparison of Extended Data Fig. 2a and Fig. 2b, where the red areas are more widespread at the first warming threshold.

The rate of change in heating and cooling needs

This section examines the linear or non-linear nature of changes in CDD and HDD across global warming levels for all countries. The earlier analysis indicates that, among the 20 countries most impacted by changes in HDD and CDD, the transition from the 1.0°C (2006–2016) to the 1.5°C warming scenario represents the most significant shift. However, a key question remains: will this short-term acceleration in HDD and CDD trends follow a similar pattern across all countries, or will regional variations emerge?

Fig. 3 answers the question, illustrating all countries' normalised changes in CDD (Fig. 3a) and HDD (Fig. 53b). It compares the CDD-HDD observations from 2006-2016, a period with a global mean temperature rise of 1.0°C, to the projected CDD-HDD scenarios, with a global mean temperature rise of 1.5°C and 2.0°C.

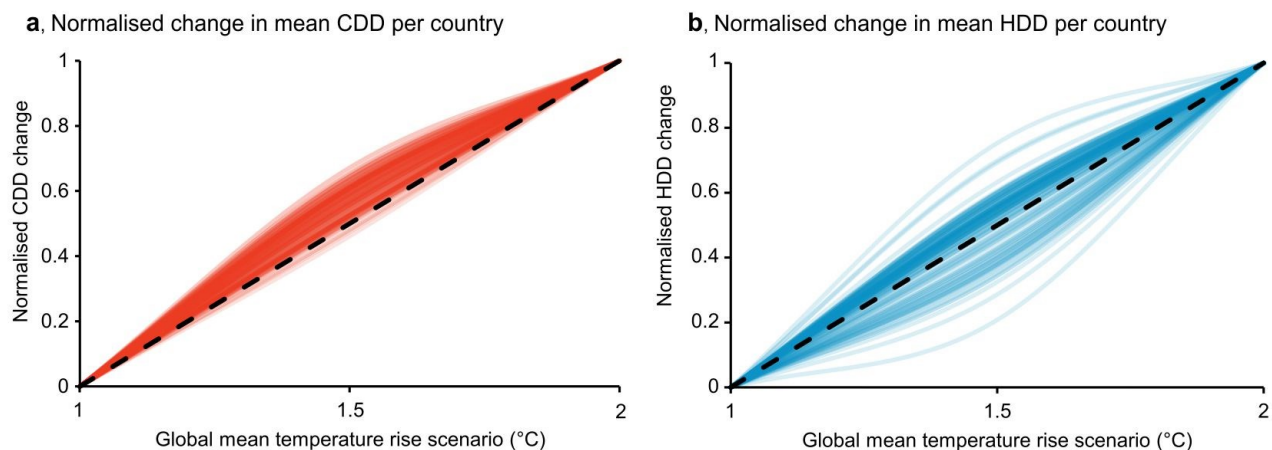


Figure 3 | Normalised changes in area-weighted mean CDD (Fig. 3a) and HDD (Fig. 3b) for all countries.

The comparison is drawn between the historical scenario — based on observations from 2006-2016, with a global mean temperature rise of 1.0°C following the HAPPI protocol²² — and the projected scenarios for a global mean temperature rise of 1.5°C and 2.0°C.

The results clearly demonstrate how the warming rate is accelerating the increase in CDD during the current decade for all countries, as the world approaches a global mean temperature rise of 1.5°C. This trend shows that even regions with historically moderate cooling demands (low CDD values) are experiencing sharper increases in CDD as temperatures rise. Consequently, this leads to a significant increase in energy demand for cooling systems, posing challenges for energy infrastructure and sustainable development. Additionally, this rapid shift underscores the need for more resilient, energy-efficient building designs and cooling technologies to mitigate the growing reliance on air conditioning systems.

In the case of HDD, results reveal a more complex and varied pattern across countries. Some countries, particularly those in colder regions, experience a notably higher decrease in HDD as temperatures warm during the current decade before the global mean temperature reaches 1.5°C, as discussed in the previous section. In contrast, other countries show the opposite trend, with less significant or delayed changes in HDD. This divergence underscores regional differences in climate sensitivity and the interplay of local geography, seasonal patterns, and baseline temperatures. Regions experiencing significant changes earlier will need to adapt their heating strategies, which may operate at partial load more frequently and for more extended periods, while those with delayed changes may have more time to adjust. These findings emphasise the importance of region-specific policies to address heating demands, improve energy efficiency, and optimise building services in response to climate change.

Implications under the SSP2-4.5 pathway

The dataset's independence from specific emissions or socioeconomic pathways enables its application in various policy and planning contexts. In this section, we explore the implications of our dataset using a specific Shared Socioeconomic Pathway (SSP) scenario as an illustrative example.

We employ SSP2-4.5, which represents a "middle-of-the-road" socioeconomic context, to illustrate how our dataset can be incorporated into a particular pathway in which global development trends follow historical trajectories (refer to Fig. 4a – orange line)²⁵. Under this scenario, the global population is projected to increase from approximately 6.81 billion in 2010 to 8.32 billion by 2030 and 9.24 billion by 2050 (Fig. 4b – orange line)^{25,26}. This example provides a concrete case for interpreting the impact of projected changes in heating and cooling demand, illustrating the relevance of our dataset for informing sectoral adaptation strategies under plausible future conditions.

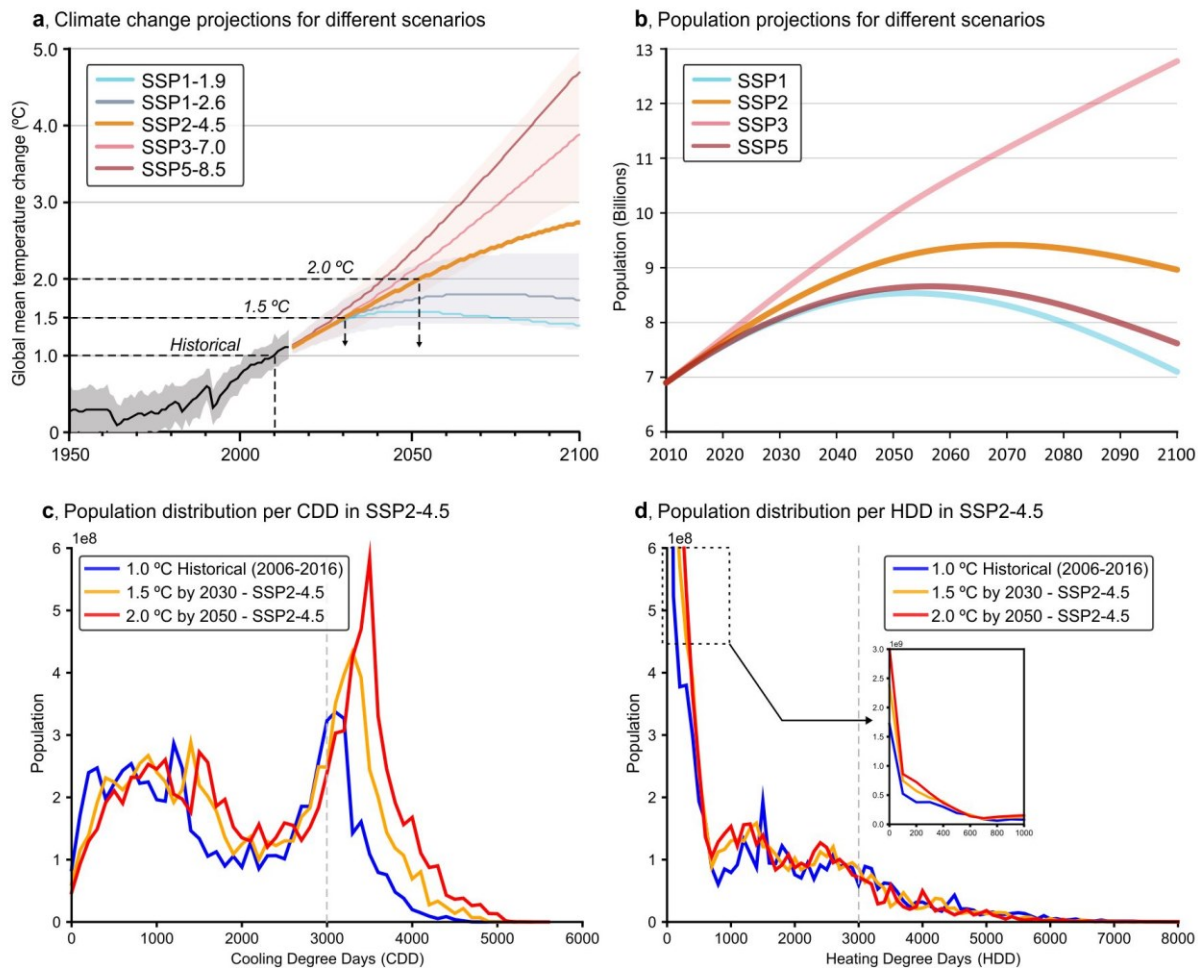


Figure 4 | Implications of CDD and HDD for the IPCC scenario SSP2-4.5. a Climate change projections across IPCC scenarios, with identification of the generated CDD and HDD datasets used for SSP2-4.5 (dashed lines). Colour shading shows the uncertainty ranges for the low and high emissions scenarios (SSP1-2.6 and

SSP3-7.0). **b**, Population projections for different Shared Socioeconomic Pathways (SSPs). **c**, Population distribution over CDD in SSP2-4.5, with the total number of population aggregated in 100 CDD intervals. **d**, Population distribution per HDD in SSP2-4.5, with the total population aggregated in 100 HDD intervals.

For this “middle-of-the-road” socioeconomic pathway (or intermediate pathway, SSP2-4.5), Figs. 4c and 4d analyse the global population's exposure to HDD and CDD under the SSP2 pathway for 1°C (historical, 2006-2016), 1.5°C, and 2.0°C scenarios. Global population data are grouped in increments of 100 CDD and HDD.

Fig. 4c shows the total distribution of the population under different heat exposures, aggregated in 100 CDD intervals. The figure highlights how people living in extreme heat regions (>3,000 CDD) are projected to increase from 23% (1.54 billion – blue line) in 2010 to 34% (2.80 billion – orange line) by 2030 and to 41% (3.79 billion – red line) by 2050. The countries with the largest populations affected by these extremes are, and will continue to be, India, Nigeria, Indonesia, Bangladesh, Pakistan, and the Philippines. Also, global people x CDD (people-CDD) is expected to increase by 42% if the global warming level reaches 1.5°C. This figure will extend to 74% if we reach 2.0°C.

From a different perspective, in SSP2-4.5, the total distribution of the population by heating need is illustrated in Fig. 4d, aggregated into 100 HDD intervals. Here, people living in extremely cool regions (>3000 HDD) are projected to decrease from 14% (0.93 billion – blue line) to 10% (0.80 billion – orange line) by 2030, and to 7% (0.68 billion – red line) by 2050. Globally, global people x HDD (people-HDD) will increase by 1% if the global warming level reaches 1.5°C, mainly due to population growth, but decrease by 4% if it reaches 2.0°C.

Discussion

The global gridded dataset of Heating and Cooling Degree Days developed in this study captures how global warming levels of 1.5 °C and 2.0 °C above pre-industrial levels influence thermal energy demand worldwide. Beyond quantifying spatial variations in heating and cooling needs, the dataset provides a foundation for assessing regional disparities in climate hazards, vulnerability, and coping capacity, offering valuable insights for adaptation planning and risk management.

The statistical analysis of the dataset also highlights several key insights of broader relevance that should be carefully considered, including the non-linear rate of increase in climate intensity, the countries most affected, and the projected increase in the number of people living under extreme heat conditions, as discussed below.

The warming rate is not linear between 1.0°C (2006-2016), 1.5°C, and 2.0°C. Cooling needs are changing faster in the current decade as the world approaches a 1.5°C global temperature rise, with CDD increases from 1.0°C to 1.5°C surpassing those expected between 1.5°C and 2.0°C. This has important implications for adaptation to warming temperatures, including the need for rigorous, immediate, sustainable solutions. In terms of heating needs, these rapid changes are particularly evident in the coolest regions.

Countries with significant implications for a global mean temperature rise of 2.0°C are also identified. Canada, the Russian Federation, Finland, Sweden, and Norway will experience a significant decrease in area-weighted mean HDD, ranging from 554 to 850 HDD, drastically reducing future heating needs per capita. Analogously, the Central African Republic, Nigeria, South Sudan, Laos, and Brazil will experience a significant rise in area-weighted mean CDD per country, increasing by 524-560 CDD, drastically increasing cooling needs per capita. The countries experiencing the most significant changes in CDD are predominantly developing nations in tropical and subtropical regions. These regions, characterised by warm year-round climates and high temperatures, are primarily found in Africa, with additional representation from South America, Central America, and Southeast Asia. As these shifts in CDD continue, they are expected to place additional pressure on the socio-economic development of these countries, exacerbating existing challenges and hindering their growth and resilience.

It should also be noted that the impact of temperature-related climate change on people, energy, infrastructure, the economy and the environment is determined not only by absolute values but also by the relative changes compared to historical conditions. This principle is particularly important for future CDD or cooling needs, especially in countries lacking the infrastructure to manage cooling demand. Given that these countries' built environment and infrastructure are predominantly prepared

for cold seasons (e.g., homes that maximise solar gains and minimise ventilation, public transport without air conditioning systems, etc.), the anticipated temperature increase, though moderate, will likely have a severe impact compared to regions with the resources, capacity and embodied capital to manage heat²³.

These findings also reveal how, under a “middle of the road” shared socioeconomic pathway scenario (SSP2-4.5), the population living in extreme heat regions (>3,000 CDD) is projected to increase from 23% (1.54 billion) in 2010 to 34% (2.80 billion) by 2030 and to 41% (3.79 billion) by 2050. The results underscore the rapidly growing vulnerability of populations to extreme heat and emphasise the need for targeted adaptation and mitigation strategies to address the impacts of rising temperatures. Additionally, they highlight that global population x CDD (people-CDD) is expected to increase by 74% if the global mean temperature increases to 2.0°C, while global population x HDD (people-HDD) is expected to decrease by 4% if we reach 2.0°C.

This open-source dataset offers valuable insights for anticipating future energy demand, optimising energy systems, and advancing climate adaptation and sustainable development goals. To ensure the practical relevance of these findings, it is essential to demonstrate how they can support decision-making across key sectors. The projections of heating and cooling degree days (HDD and CDD) can be directly applied to inform early-stage building design, regional energy system planning, and public health preparedness.

For instance, in the building sector, the gridded HDD and CDD data can guide climate-responsive planning by identifying regions where cooling demand is projected to increase most significantly in the coming decades²⁷. In areas shifting from heating-dominated to mixed or cooling-dominated climates, architects and engineers can prioritise adaptation strategies for sustainable cooling²⁸—such as shading, ventilation, or thermal mass—and revise building standards to align with emerging needs.

In energy system planning, spatially resolved HDD and CDD trends offer critical inputs for forecasting future energy loads, enabling planners and utilities to anticipate changes in peak demand and to consider centralised and/or decentralised energy solutions, such as demand flexibility^{29,30} or district heating and cooling networks³¹. These data are beneficial for scenario analysis and long-term planning at both the regional and national levels.

From a public health perspective, rising CDD values highlight regions at growing risk of extreme heat exposure, especially in areas with historically low cooling demand. These insights can support the design of heat-health early warning systems, the strategic placement of cooling shelters, and the development of heatwave response plans—particularly in regions with vulnerable populations³².

By applying these metrics across disciplines, stakeholders can better prepare for climate-induced changes in temperature patterns, supporting more resilient and adaptive systems.

Methods

In this section, we describe the data and methods used to generate the global gridded maps of CDD and HDD and perform the geospatial statistical analysis.

Climate data and selection criteria

The global gridded CDD and HDD maps were generated using a large bias-corrected HadAM4-based temperature ensemble for three global warming levels (1°C, 1.5°C and 2.0°C) generated by Lizana et al. (2024)¹⁷ and available at the CEDA repository¹⁸. This climate dataset was produced using the HadAM4 Atmosphere-only General Circulation Model (AGCM)^{33,34} from the UK Met Office Hadley Centre. The simulations were conducted within the climateprediction.net (CPDN) climate modelling environment²⁰, which employs the Berkeley Open Infrastructure for Network Computing (BOINC) framework to distribute numerous computational tasks across a global network of volunteer computers

This temperature ensemble was chosen for four reasons: (1) its large ensemble size of 70 members over ten years per scenario, (2) its high spatiotemporal resolution with 6-hourly mean temperatures at $0.883^\circ \times 0.556^\circ$, (3) its bias-corrected simulations, and (4) its capability to represent global mean temperature rise scenarios by 1.5°C and 2.0°C independently of when these thresholds are achieved (3). This ensemble size is significantly larger than those typically available in other model intercomparison projects (e.g., CMIP6), where most models provide only 10–30 ensemble members per scenario. The use of the HadAM4 model within the CPDN framework also allows for output at a 6-hourly temporal resolution, significantly finer than the daily output commonly available from recent climate model ensembles. Also, the model focuses on global mean temperature rise levels of 1.5°C and 2.0°C, independent of when or under which pathway these temperature thresholds are reached. This framing enables a policy-relevant, scenario-agnostic assessment of climate impacts that aligns directly with the temperature goals of the Paris Agreement. The climate modelling aligns with the HAPPI protocol, which prescribes constant forcing levels consistent with 1.5°C and 2.0°C of global warming above pre-industrial levels. All ensemble members were run with these fixed forcings over a 10-year period to sample the climate system's internal variability. Consequently, the simulations are not designed to reach 1.5 °C or 2.0 °C at a specific point in time; rather, they represent stabilised climate states corresponding to these warming levels. Any temporal differences observed across ensemble members reflect internal model variability, not differences in when the warming thresholds were reached.

Bias correction

The temperature ensembles generated by Lizana et al. (2024)¹⁷ were corrected for bias using a quantile-mapping method, which adjusts the full distribution of modelled temperatures to match observed data. This method corrects systematic biases at each percentile, ensuring a representation of both average conditions and extremes while preserving the ensemble's internal variability. For this process, the ERA5 reanalysis dataset^{35,36} with a spatial resolution of 0.25° was re-gridded to a 0.833° × 0.556° grid to match the model resolution. Biases were calculated at each percentile by comparing the cumulative distribution functions of the historical model output and ERA5 observations. The calculated biases were added to the 1 °C (2006–2016), 1.5 °C, and 2.0 °C temperature scenarios at their corresponding percentiles, assuming that the bias remains constant across scenarios. The bias correction was applied to the combined ensemble, comprising 70 individual members over a 10-year period, thereby preserving the internal variability of the multi-member ensemble after correction. More details can be found in Lizana et al. (2024)¹⁷.

Validation and uncertainty

The validation and reliability of the bias-corrected HadAM4-based temperature ensemble used in this study were assessed by comparing the bias-corrected HadAM4-based temperature ensemble with ERA5 (for the historical period between 2006 and 2016) and with the CMIP6 multi-model mean for future projections¹⁷. Details from this analysis are provided in SN6. The analysis shows that the ensemble used to generate the historical maps aligns perfectly with ERA5 observations, indicating the good performance of the bias-corrected historical model output. Comparing future projections for 1.5°C and 2.0°C scenarios with the CMIP6 model mean shows similar overall warming, with most temperature differences within ±0.5°C and slightly higher warming (0.5–1°C) in some high northern latitudes. These differences are within the range of differences seen between other models and lie within the range of credible projections produced by contemporary climate models³⁷.

Other datasets used

Other datasets were used to provide an example on how to use this dataset under a specific Shared Socioeconomic Pathway (SSP) scenario: the SSP2-4.5 pathway defined by IPCC (2022)²⁵. The global gridded population datasets for this SSP2-4.5 scenario across different temporal periods were obtained from Wang et al.³⁸ and are available in the figshare repository³⁹. These datasets were used to quantify the implications of CDD and HDD in the population, illustrated in Fig. 4.

Calculation of Heating Degree Days and Cooling Degree Days

HDD and CDD measure how much the dry-bulb temperature exceeds (above or below) a reference temperature threshold ($T_{Threshold}$) each day over a given period.

The calculation of HDD and CDD can follow different methodologies depending on the available data, context, and intended application⁸. Commonly used reference temperature thresholds for calculating HDD and CDD are 65 °F (18.0 °C)^{4,40–43}. Some studies adopt 18.3 °C as a direct conversion from 65 °F^{9,15}, while others apply even higher thresholds^{9,42}. Temperature data used in these calculations may vary in temporal resolution, from daily to sub-daily records. Although finer resolutions tend to improve accuracy, the difference between daily and hourly estimates is usually minor⁸.

In this study, HDD and CDD are calculated using 6-hourly temperature data following the approach previously used in Nicole et al. (2023)²³ and described in Eqs. (1) and (2). This sub-daily resolution captures part of the diurnal temperature variability, which is particularly important in regions with large day–night temperature ranges. Both $T_{threshold}$ and T_{base} were set to 18 °C.

$$HDD = \frac{\sum_{t=0}^{t=m} (T_{base} - T_t)}{n}, T_t < T_{threshold} \quad (1)$$

$$CDD = \frac{\sum_{t=0}^{t=m} (T_t - T_{base})}{n}, T_t > T_{threshold} \quad (2)$$

Where:

t = time step

m = last time step of the year

n = number of time steps in one day ($n = 4$ for 6-hourly data)

T_t = mean outdoor temperature at time t

T_{base} = reference temperature used to calculate the temperature difference.

$T_{threshold}$ = outdoor temperature above which temperature differences are calculated.

Global gridded maps of HDD and CDD

The global gridded maps of HDD and CDD were obtained as follows. First, HDD and CDD were calculated annually across 700 annual periods per scenario (70 temperature members per scenario over a 10-year period). Here, we obtained 700 CDD and HDD global gridded maps per global warming level: 1.0°C (historical, 2006-16), 1.5°C and 2.0°C above pre-industrial levels. Second, five statistical indices across these large ensembles of HDD and CDD are obtained per coordinate (long x lat) and scenario to capture the climate variability. These statistical indices are mean, median, 10th percentile, 90th percentile, and standard deviation. Third, the final statistical results of HDD and CDD were stored in five different global gridded maps per scenario as NetCDF V4 files (*.nc). These global gridded maps have a spatial resolution of 0.833° x 0.556° (longitude x latitude) over the land surface and are available at the ORA repository²⁴.

Geospatial statistics and visualisation

The spatial visualisations and area-weighted statistics for each sub-region and country presented in this manuscript were produced utilising Python programming and the QGIS geographic information system. The Python code is available on GitHub (https://github.com/lizanafj/python_examples_with_CDDandHDD_files). The administrative boundaries used to perform these geospatial statistics were obtained from EuroGeographics and Natural Earth. Area-weighted statistics for all countries with populations exceeding 2 million are detailed in the Supplementary Information (see SN3 and SN4).

Limitations

HDD and CDD were calculated using the dry bulb temperature, following the standard approach to enable comparison with previous studies⁸. These indices are directly related to heat and cooling exposure but do not account for other social, economic, and environmental factors influencing heating and cooling energy demand. These factors include the existing building stock and its thermal performance, socio-technical behaviours and usage patterns, access to energy resources, the availability of heating and cooling technologies, and other variables influencing thermal comfort, such as humidity.

The dataset was generated from HadAM4 climate model outputs. HadAM4 lacks interactive coupling to ocean and aerosol components. When compared with the CMIP6 multi-model mean, most temperature differences are below ± 0.5 °C and the largest differences, generally within 0.5–1 °C, occurring in mid-to-high northern latitudes. The greater warming projected by HadAM4 may lead to underestimation of HDD and overestimation of CDD in these regions, indicating a potential warm bias in derived indicators. However, these differences remain within the range observed among other models and lie within the credible projections produced by contemporary climate models³⁷. It is also important to note that direct comparisons between HadAM4 and CMIP6 ensembles should be interpreted with caution, as differences in ensemble size, temporal sampling, and model formulation can influence the results. Further details are provided in the SN6.

Additionally, since the global climate dataset used does not account for urban heat island (UHI) effects, HDD values are likely overestimated and CDD values are underestimated in urban areas.

The use of other datasets associated with SSP2-4.5 served to demonstrate how our CDD and HDD datasets can be integrated into a “middle-of-the-road” socioeconomic context. It is important to note, however, that the SSP2-4.5 projections carry inherent uncertainties (e.g. regional downscaling methods), which should be considered when interpreting the results.

Data availability

The global gridded dataset of HDD and CDD under the three climate change scenarios (1°C, 1.5°C and 2°C) is available in the Oxford University Research Archive (ORA) repository at (<https://ora.ox.ac.uk/objects/uuid:6fced8c0-5c64-44af-b38e-e99785b2db90>) or (<https://doi.org/10.5287/ora-w4qpqy522>). Five maps are available for HDD and CDD per scenario: mean, median, 10th percentile, 90th percentile, and standard deviation. The complete list of maps for each global warming level is provided in Extended Data Table 1. The spatial resolution is 0.833° x 0.556° (longitude x latitude) over the land surface. Further data are available from the authors on request.

Code availability

The code to calculate HDD and CDD from the temperature ensemble is available at https://github.com/lizanafj/cdd_hdd_mapping. The code for data visualisation and statistical analysis can be found at https://github.com/lizanafj/python_examples_with_CDDandHDD_files. Examples of how to use the Python code are provided in SN7.

Acknowledgements

This research received support from the University of Oxford Strategic Research Fund and the Oxford Martin School's Future of Cooling Programme. J.L. acknowledges funding from the European Union's Horizon 2020 research and innovation programme [MSCA: 101023241]. S.S. was funded by UKRI [NE/P002099/1]. To ensure open access, the author has granted a CC BY licence to any Author Accepted Manuscript resulting from this work. The authors are also grateful to Miriam Zachau Walker and Renaldi Renaldi for their valuable contributions to the early stages of the research concept.

Author contributions

R.K., D.C.H.W. and M.M. conceptualised the work proposed. J.L. and N.M. coordinated the study. N.M. performed the data extraction and data management. J.L. performed the data pre-processing of the climate model. J.L. calculated and generated the CDD and HDD datasets. J.L. provided the statistics and visualisations available in the manuscript. J.L. wrote the manuscript draft. S.S. and D.C.H.W. led the interpretation and analysis of the data. S.S. provided expertise in data analytics. All authors reviewed the paper.

Competing interests

The authors have no competing interests to declare.

Additional information

Supplementary information is available for this paper.

SN 1: Global gridded dataset of HDD and CDD. List of files.

SN 2: Illustration of mean HDD and CDD maps.

SN 3: Supplementary ranking of countries by area-weighted mean HDD.

SN 4: Supplementary ranking of countries by area-weighted mean CDD.

SN 5: Descriptive statistics of the complete HDD and CDD dataset.

SN 6: Comparison of HadAM4-based ensemble with other multi-model ensembles.

SN 7: Code examples in Python for multi-scale data analysis.

References

1. IPCC. Chapter 9: Buildings. in *Climate Change 2022 - Mitigation of Climate Change* (ed. [P.R. Shukla, J. Sk[P.R. Shukla, J. Skea, R. Slade, A. Al Khourdajie, R. van Diemen, D. McCollum, M. Pathak, S. Some, P. Vyas, R. Fradera, M. Belkacemi, A. Hasija, G. Lisboa, S. Luz, J. Malley, (eds.)ea, R. Slade, A. Al Khourdajie, R. van Diemen, D. McCol, (eds.)]) 953–1048 (Cambridge University Press, 2023). doi:10.1017/9781009157926.011.
2. Khosla, R. *et al.* Cooling for sustainable development. *Nature Sustainability* **4**, 201–208 (2021).
3. IEA. Is cooling the future of heating? 2020 <https://www.iea.org/commentaries/is-cooling-the-future-of-heating>.
4. IEA. *The Future of Cooling. Opportunities for energy-efficient air conditioning*. (IEA Publications, 2018).
5. Reinhart, C. Linking energy use to local climate. *Nature Energy* **8**, 1311–1312 (2023).
6. UNEP. *Global Status Report for Buildings and Construction: Beyond foundations: Mainstreaming sustainable solutions to cut emissions from the buildings sector*. (2024) doi:10.59117/20.500.11822/45095.
7. Staffell, I., Pfenninger, S. & Johnson, N. A global model of hourly space heating and cooling demand at multiple spatial scales. *Nature Energy* (2023) doi:10.1038/s41560-023-01341-5.
8. CIBSE. *Degree-Days: Theory and Application - TM41 : 2006*. (CIBSE, 2006).
9. Biardeau, L. T., Davis, L. W., Gertler, P. & Wolfram, C. Heat exposure and global air conditioning. *Nature Sustainability* **3**, 25–28 (2020).
10. Mistry, M. N. Historical global gridded degree-days: A high-spatial resolution database of CDD and HDD. *Geoscience Data Journal* **6**, 214–221 (2019).
11. Petri, Y. & Caldeira, K. Impacts of global warming on residential heating and cooling degree-days in the United States. *Scientific Reports* **5**, 12427 (2015).
12. Spinoni, J. *et al.* Changes of heating and cooling degree-days in Europe from 1981 to 2100. *International Journal of Climatology* **38**, e191–e208 (2018).
13. Almazroui, M., Saeed, S., Saeed, F., Islam, M. N. & Ismail, M. Projections of Precipitation and Temperature over the South Asian Countries in CMIP6. *Earth Systems and Environment* **4**, 297–320 (2020).
14. Almazroui, M. *et al.* Projected Change in Temperature and Precipitation Over Africa from CMIP6. *Earth Systems and Environment* **4**, 455–475 (2020).
15. Deroubaix, A. *et al.* Large uncertainties in trends of energy demand for heating and cooling under climate change. *Nature Communications* 2021 12:1 **12**, 1–8 (2021).
16. Spinoni, J. *et al.* Global population-weighted degree-day projections for a combination of climate and socio-economic scenarios. *International Journal of Climatology* **41**, 5447–5464 (2021).
17. Lizana, J. *et al.* Ensemble of global climate simulations for temperature in historical, 1.5 °C and 2.0 °C scenarios from HadAM4. *Scientific Data* **11**, 578 (2024).
18. Lizana, J. *et al.* Large ensemble of global mean temperatures: 6-hourly HadAM4 model run data using the Climateprediction.net platform. (2023) doi:10.5285/9c41e3aa67024bbdad796290a861e968.
19. Watson, P. *et al.* Multi-thousand member ensemble atmospheric simulations with global 60km resolution using climateprediction.net. *Technical Report EGU2020-10895*. Copernicus

- Meetings* (2020) doi:10.5194/egusphere-egu2020-10895.
20. Climateprediction.net (CPDN) program. <https://www.climateprediction.net/>.
 21. Leach, N. J., Watson, P. A. G., Sparrow, S. N., Wallom, D. C. H. & Sexton, D. M. H. Generating samples of extreme winters to support climate adaptation. *Weather and Climate Extremes* **36**, 100419 (2022).
 22. Mitchell, D. *et al.* Half a degree additional warming, prognosis and projected impacts (HAPPI): background and experimental design. *Geoscientific Model Development* **10**, 571–583 (2017).
 23. Miranda, N. D. *et al.* Change in cooling degree days with global mean temperature rise increasing from 1.5 °C to 2.0 °C. *Nature Sustainability* **6**, 1326–1330 (2023).
 24. Lizana, J. *et al.* Global land surface dataset of Heating and Cooling Degree Days from a bias-corrected HadAM4-based temperature ensemble under 1.0°C, 1.5°C, and 2.0°C climate scenarios. (2024) doi:10.5287/ora-w4qpqy522.
 25. IPCC. *Climate Change 2022: Impacts, Adaptation, and Vulnerability. Contribution of Working Group II to the Sixth Assessment Report of the Intergovernmental Panel on Climate Change*. (Cambridge University Press, 2022). doi:10.1017/9781009325844.
 26. KC, S. & Lutz, W. The human core of the shared socioeconomic pathways: Population scenarios by age, sex and level of education for all countries to 2100. *Global Environmental Change* **42**, 181–192 (2017).
 27. Mehmood, S., Lizana, J., Núñez-Peiró, M., Maximov, S. A. & Friedrich, D. Resilient cooling pathway for extremely hot climates in southern Asia. *Applied Energy* **325**, 119811 (2022).
 28. Lizana, J. *et al.* Overcoming the incumbency and barriers to sustainable cooling. *Buildings and Cities* **3**, 1075–1097 (2022).
 29. Franken, L. *et al.* Power system benefits of simultaneous domestic transport and heating demand flexibility in Great Britain’s energy transition. *Applied Energy* **377**, 124522 (2025).
 30. Halloran, C., Lizana, J., Fele, F. & McCulloch, M. Data-based, high spatiotemporal resolution heat pump demand for power system planning. *Applied Energy* **355**, 122331 (2024).
 31. Lizana, J., Ortiz, C., Soltero, V. M. & Chacartegui, R. District heating systems based on low-carbon energy technologies in Mediterranean areas. *Energy* **120**, 397–416 (2017).
 32. Ballester, J. *et al.* Heat-related mortality in Europe during the summer of 2022. *Nature Medicine* **29**, 1857–1866 (2023).
 33. Webb, M., Senior, C., Bony, S. & Morcrette, J.-J. Combining ERBE and ISCCP data to assess clouds in the Hadley Centre, ECMWF and LMD atmospheric climate models. *Climate Dynamics* **17**, 905–922 (2001).
 34. Williams, K. D., Ringer, M. A. & Senior, C. A. Evaluating the cloud response to climate change and current climate variability. *Climate Dynamics* **20**, 705–721 (2003).
 35. Hersbach, H. *et al.* ERA5 hourly data on single levels from 1940 to present. (2023) doi:10.24381/cds.adbb2d47.
 36. ECMWF. ERA5 hourly data on single levels from 1959 to present. <https://cds.climate.copernicus.eu/cdsapp#!/dataset/reanalysis-era5-single-levels?tab=overview>.
 37. Wehner, M. *et al.* Changes in extremely hot days under stabilized 1.5 and 2.0 °C global warming scenarios as simulated by the HAPPI multi-model ensemble. *Earth System Dynamics* **9**, 299–311 (2018).

38. Wang, X., Meng, X. & Long, Y. Projecting 1 km-grid population distributions from 2020 to 2100 globally under shared socioeconomic pathways. *Scientific Data* **9**, 1–13 (2022).
39. Wang, X., Meng, X. & Long, Y. Projecting 1 km-grid population distributions from 2020 to 2100 globally under shared socioeconomic pathways. (2022) doi:10.6084/m9.figshare.19608594.v2.
40. Labriet, M. *et al.* Worldwide impacts of climate change on energy for heating and cooling. *Mitigation and Adaptation Strategies for Global Change* **20**, 1111–1136 (2015).
41. Isaac, M. & van Vuuren, D. P. Modeling global residential sector energy demand for heating and air conditioning in the context of climate change. *Energy Policy* **37**, 507–521 (2009).
42. Andrijevic, M., Byers, E., Mastrucci, A., Smits, J. & Fuss, S. Future cooling gap in shared socioeconomic pathways. *Environmental Research Letters* **16**, (2021).
43. Sivak, M. Where to live in the United States: Combined energy demand for heating and cooling in the 50 largest metropolitan areas. *Cities* **25**, 396–398 (2008).

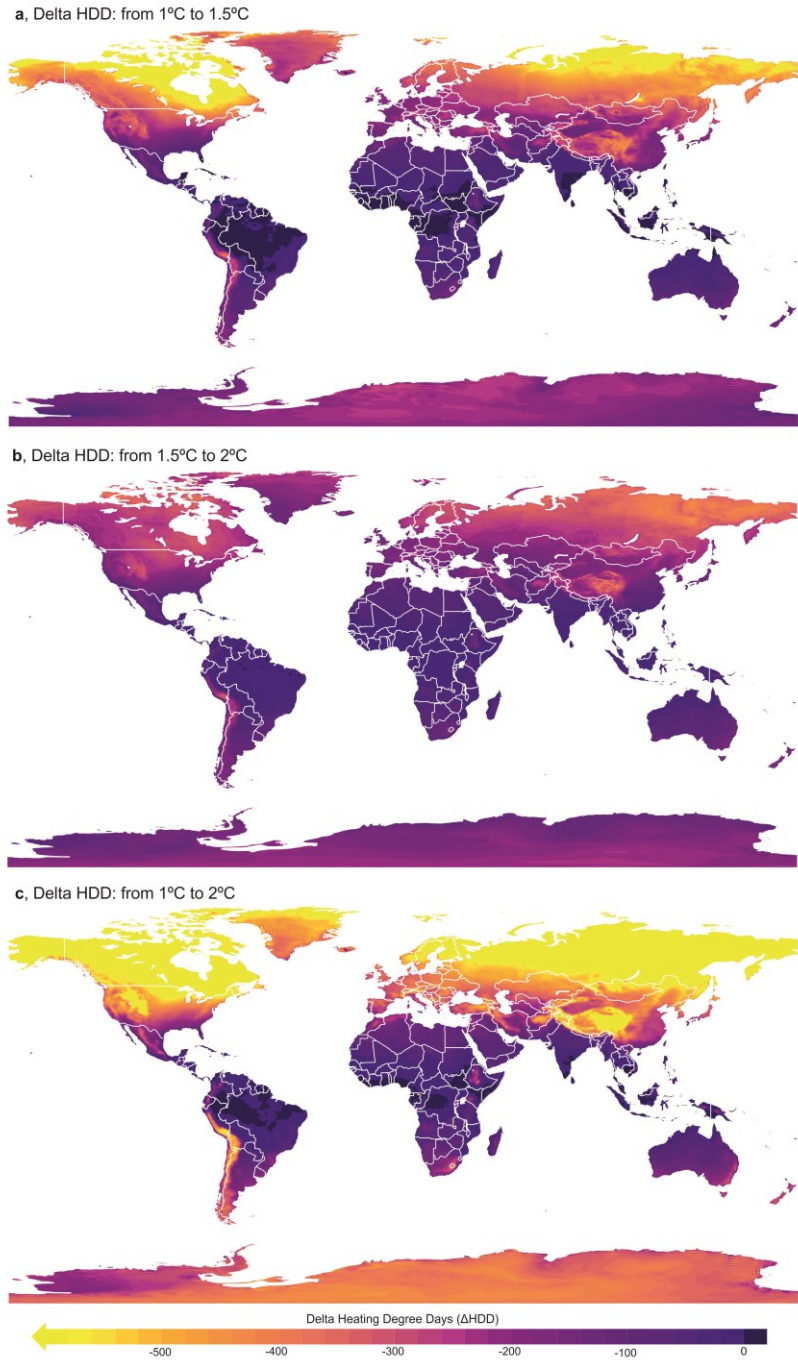
Extended data

Extended Data Table 1 | Overview of the global gridded maps of HDD and CDD by warming scenario. This table lists the global gridded maps generated for three climate change scenarios: 1.0°C, 1.5°C, and 2.0°C. For each variable and scenario, five statistical descriptors of the model ensemble are provided: mean, median, 10th percentile, 90th percentile, and standard deviation. These metrics were calculated from annual CDD and HDD values derived from a temperature ensemble comprising 70 members over a 10-year period, representing a total of 700 simulated years per scenario.

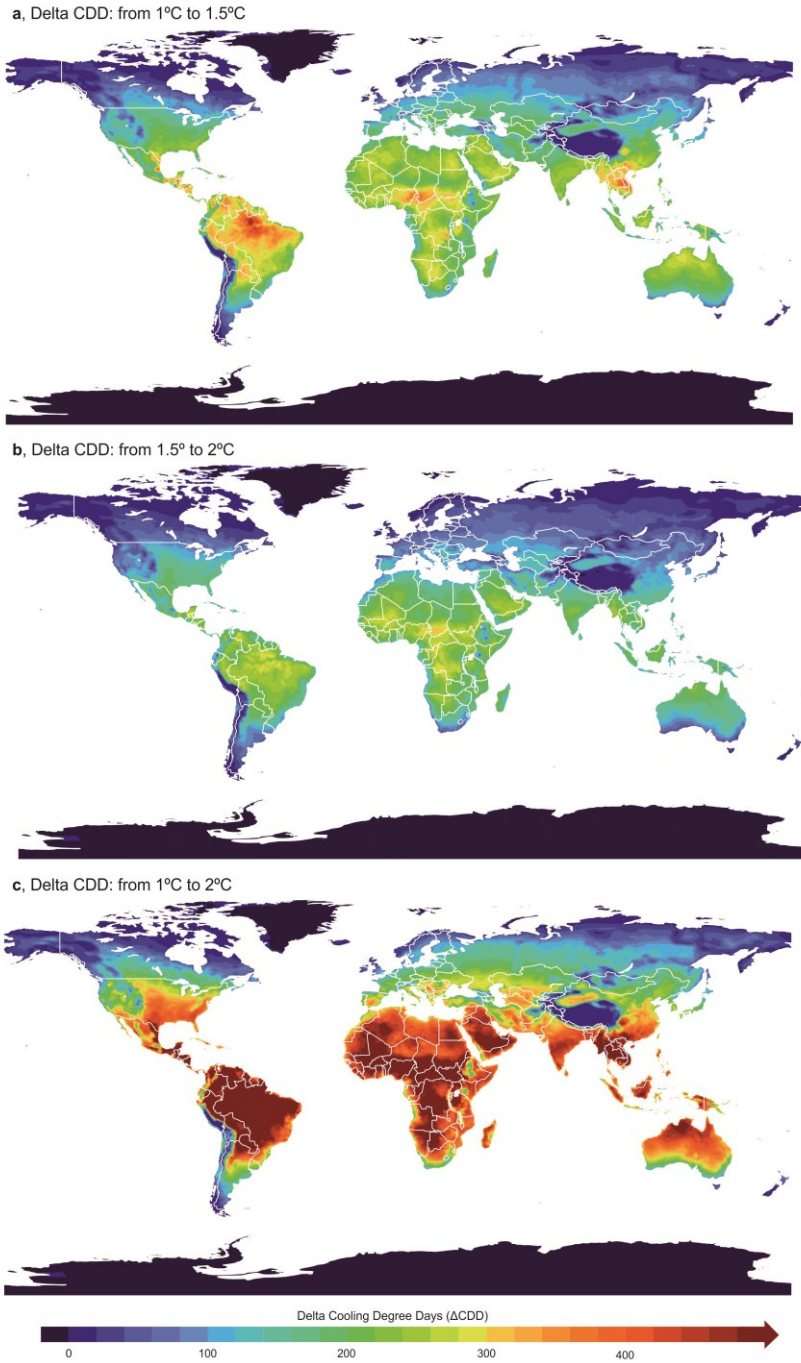
Maps/Variable	Resolution ^a	Temporal domain ^b	File type	Minimum	10 th percentile	Median	90 th percentile	maximum
HEATING DEGREE DAYS								
1.0°C scenario								
Mean HDD	0.833° × 0.556°	2006-2016	NetCDF V4	0	32	6971	22493	25453
Median HDD	0.833° × 0.556°	2006-2016	NetCDF V4	0	30	6932	22525	25358
10th percentile HDD	0.833° × 0.556°	2006-2016	NetCDF V4	0	14	6362	21904	24972
90th percentile HDD	0.833° × 0.556°	2006-2016	NetCDF V4	0	52	7638	23106	26096
Standard deviation HDD	0.833° × 0.556°	2006-2016	NetCDF V4	0	12	240	361	539
1.5°C scenario								
Mean HDD	0.833° × 0.556°	-	NetCDF V4	0	28	6555	22286	25230
Median HDD	0.833° × 0.556°	-	NetCDF V4	0	20	6508	22298	25228
10th percentile HDD	0.833° × 0.556°	-	NetCDF V4	0	4	5430	21206	24175
90th percentile HDD	0.833° × 0.556°	-	NetCDF V4	0	60	7749	23361	26355
Standard deviation HDD	0.833° × 0.556°	-	NetCDF V4	0	20	409	588	814
2.0°C scenario								
Mean HDD	0.833° × 0.556°	-	NetCDF V4	0	19	6297	22096	25040
Median HDD	0.833° × 0.556°	-	NetCDF V4	0	12	6258	22125	25046
10th percentile HDD	0.833° × 0.556°	-	NetCDF V4	0	2	5190	20980	23961
90th percentile HDD	0.833° × 0.556°	-	NetCDF V4	0	43	7469	23178	26158
Standard deviation HDD	0.833° × 0.556°	-	NetCDF V4	0	16	412	590	812
COOLING DEGREE DAYS								
1.0°C scenario (2006-2016)								
Mean CDD	0.833° × 0.556°	2006-2016	NetCDF V4	0	0	78	2904	5125
Median CDD	0.833° × 0.556°	2006-2016	NetCDF V4	0	0	73	2890	5121
10th percentile CDD	0.833° × 0.556°	2006-2016	NetCDF V4	0	0	43	2701	4924
90th percentile CDD	0.833° × 0.556°	2006-2016	NetCDF V4	0	0	115	3105	5308
Standard deviation CDD	0.833° × 0.556°	2006-2016	NetCDF V4	0	0	25	109	217
1.5°C scenario								
Mean CDD	0.833° × 0.556°	-	NetCDF V4	0	0	128	3160	5329
Median CDD	0.833° × 0.556°	-	NetCDF V4	0	0	108	3144	5323
10th percentile CDD	0.833° × 0.556°	-	NetCDF V4	0	0	37	2703	4805
90th percentile CDD	0.833° × 0.556°	-	NetCDF V4	0	0	241	3654	5847
Standard deviation CDD	0.833° × 0.556°	-	NetCDF V4	0	0	71	216	394
2.0°C scenario								
Mean CDD	0.833° × 0.556°	-	NetCDF V4	0	0	161	3367	5547
Median CDD	0.833° × 0.556°	-	NetCDF V4	0	0	139	3351	5545
10th percentile CDD	0.833° × 0.556°	-	NetCDF V4	0	0	51	2892	5037
90th percentile CDD	0.833° × 0.556°	-	NetCDF V4	0	0	293	3876	6062
Standard deviation CDD	0.833° × 0.556°	-	NetCDF V4	0	0	81	227	402

^aAverage spatial resolution at mid-latitudes (~45°) is approximately 60km².

^bThe temporal domain of the projections for 1.5°C and 2.0°C is independent of specific timelines or emission pathways, thereby enabling a scenario-independent evaluation explicitly aligned with the temperature targets of the Paris Agreement.



Extended Data Figure 1 | Global changes in HDD between 1.0°C (historical, 2006-2016), and future 1.5°C and 2.0°C global warming levels. a, Absolute change in HDD (Delta HDD) between the 1.0°C and 1.5°C scenario. **b,** Absolute change in HDD (Delta HDD) between 1.5°C and 2.0°C. **c,** Absolute change in HDD (Delta HDD) between 1.0°C and 2.0°C. Delta HDD (Δ HDD) refers to the incremental/decremental change in mean annual HDD per grid. Administrative boundaries were used from EuroGeographics.



Extended Data Figure 2 | Global changes in CDD between 1.0°C (historical, 2006-2016), and future 1.5°C and 2.0°C global warming levels. a, Absolute change in CDD (Delta CDD) from 1.0°C to 1.5°C scenario. **B,** Absolute change in CDD (Delta CDD) from 1.5°C to 2.0°C scenario. **c,** Absolute change in CDD (Delta CDD) between 1.0°C and 2.0°C. Delta CDD (Δ CDD) refers to the incremental/decremental change in mean annual CDD per grid. Administrative boundaries were used from EuroGeographics.